Electron and hole effective masses from magnetoluminescence studies of modulation-doped InP/$In_{0.53}Ga_{0.47}As$ heterostructures

Q. X. Zhao, P. O. Holtz, B. Monemar, and T. Lundström
Department of Physics and Measurement Technology, Linköping University, S-581 83 Linköping, Sweden

J. Wallin and G. Landgren
Swedish Institute of Microelectronics, P.O. Box 1084, 16421 Kista, Sweden

(Received 8 February 1993; revised manuscript received 28 June 1993)

Two-dimensional (2D) carrier-recombination processes in modulation-doped unstrained InP/$In_{0.53}Ga_{0.47}As$ heterostructures with 500-Å-wide $In_xGa_{1-x}As$ active layers have been investigated with magneto-optical spectroscopy. Photoluminescence bands related to the 2D confined carriers have been observed in both *n*- and *p*-type modulation-doped structures. For the *n*-type structures it is found that the emissions observed are transitions between 2D electrons at the interface potentials and holes in the $In_xGa_{1-x}As$ valence band. Excitonic effects are not observed, even for the emission related to the third confined electronic state. For the *p*-type structures the transitions occur across the $In_xGa_{1-x}As$ layer between 2D holes and 2D electrons at the opposite interface notch potentials. Both the *n*- and the *p*-type modulation-doped structures show well-resolved Landau-level splitting when a magnetic field is applied parallel to the growth direction. The effective masses of both 2D electrons and 2D holes confined in the $In_xGa_{1-x}As$ layer are *simultaneously* obtained by analysis of the *same magneto-optical data.* Effective-mass values of $m_e=(0.054\pm0.005)m_0$ for the first subband electrons and $m_{hh}=(0.463\pm0.005)m_0$ for the first subband heavy holes, respectively, are derived from our spectra. The effective mass of $n=2$ subband electrons was found to be about 9% larger than the effective mass of $n=1$ electrons.

INTRODUCTION

Semiconductor heterostructures are very important for basic studies of the electron and hole systems in quasi-two-dimensional structures. Such systems also have a large potential for various optoelectric device applications. Many detailed optical studies have been reported for *n*-type $Al_xGa_{1-x}As$/GaAs heterostructures.[1–6] Different emissions related to confined two-dimensional (2D) electrons, such as band to band, band to impurity, exciton, and Fermi-edge singularity recombination, are observed. The optical properties of these emission bands such as spectral shape, position, lifetime, etc., have been extensively investigated.[3–6] On the other hand, the properties of 2D carriers in heterojunctions with large electron-hole spatial separation have been significantly less studied in the modulation-doped InP/$In_xGa_{1-x}As$ system.[7,8] Instead most studies on this system have been concentrated on more narrow, undoped[9–15] or modulation-doped,[16] quantum-well (QW) structures. Even though there has been a large effort concerning investigations on the effective masses of electrons and holes, there is a considerable scatter in the experimental values reported. Besides this, the experimentally determined effective masses were mostly based on different experimental conditions and different sample structures for electrons and holes, respectively. This means that the accuracy of the estimate for the effective mass of one electronic particle is dependent on the accuracy of the estimate of the effective mass for the second electronic particle.

The previous studies on 700- and 800-Å-wide *n*-type modulation-doped InP/$In_xGa_{1-x}As$ structures[7,8] have been concentrated on the magneto-optical pinning effects of Landau levels between the two interfaces and the radiative recombination mechanism. In our present study, both *p*-type and *n*-type modulation-doped InP/$In_{0.53}Ga_{0.47}As$ heterostructures with a 500-Å-wide active layer have been used. Radiative emissions related to the 2D carriers are observed in these InP/$In_xGa_{1-x}As$ structures. When a static magnetic field is applied parallel to the growth direction, a well-resolved Landau-level splitting is observed. The electron and heavy-hole effective masses have been deduced simultaneously directly from our experimental results. Magneto-optical data show that the observed transitions are mainly due to band-to-band transitions, and the exciton effects are very weak in our samples.

SAMPLES AND EXPERIMENTAL SETUP

The samples used were grown by metal-organic vapor phase epitaxy (MOVPE) on iron-doped (10^{16} cm^{-3}), semi-insulating InP substrates. The layer structure in the samples was as follows: a buffer layer of 500-nm intentionally undoped InP (*n*-type background doping at a level of about 1×10^{15} cm^{-3}), a channel layer of 50-nm unstrained $In_{0.53}Ga_{0.47}As$, a spacer layer of 10-nm undoped InP, and finally a doped layer of 50-nm InP, either *n*-type or *p*-type to a doping level of about 2×10^{18} cm^{-3}. The carrier concentrations in the well are about 8.5×10^{11} cm^{-2} for *n*-type and 9.5×10^{11} cm^{-2} for *p*-type structures

at dark conditions, estimated from microwave absorption measurements.

Photoluminescence (PL) from the samples was dispersed by a Jobin-Yvon double monochromator and relocate detected with a liquid-nitrogen-cooled North-Coast E0817 Ge detector. PL measurements were also performed in the presence of a magnetic field. The samples were then mounted in a 16-T magnet. The laser was coupled to the samples via optical fibers, and the emissions from the sample were collected through the same fiber into the monochromator. The excitation photon energy is in all cases above the InP band gap.

RESULTS AND DISCUSSIONS

An $In_{0.53}Ga_{0.47}As$ layer is lattice matched to InP. The band-gap difference between $In_{0.53}Ga_{0.47}As$ ($E_g = 0.812$ eV) (Ref. 17) and InP ($E_g = 1.424$ eV) (Ref. 18) is 0.612 eV at 2 K. The valence-band energy offset for this material system is 0.37 eV,[19] and the energy offset of the conduction band is consequently 0.242 eV at 2 K. Both the conduction band and the valence band, therefore, have fairly high potential barriers as seen from the lower band-gap $In_xGa_{1-x}As$ layer.

Figure 1 shows a schematic diagram of the band structure for both the n-type [Fig. 1(a)] and the p-type [Fig. 1(b)] modulation-doped $InP/In_{0.53}Ga_{0.47}As$ heterostructures studied in this work. Since the layers are grown on the InP buffer layer, which is slightly n-type, a quasi-triangular "notch" potential at the interface between the buffer and the 500-Å $In_xGa_{1-x}As$ layer is also formed. For the n-type structures photocreated holes are mainly located in the central region of the 500-Å $In_xGa_{1-x}As$ layer between the two interfaces, while electrons are confined at both interfaces. The possible recombination processes are indicated in Fig. 1(a). For the p-type structures $2D$ holes were confined at the interface towards the surface layer, since the surface InP layer is highly p-type doped (with 10^{18} cm^{-3} Zn impurities). The optically created electrons, on the other hand, are accumulated at the interface towards the buffer, since the buffer layer is slightly n-type (with 10^{15} cm^{-3} background impurities). The band structure and possible recombination processes for the p-type modulation-doped heterostructures are shown in Fig. 1(b).

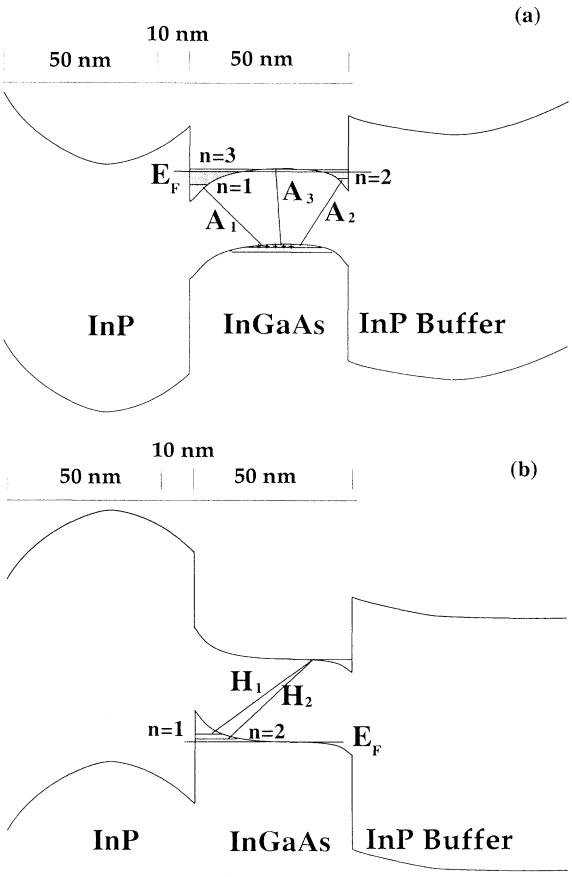

FIG. 1. Schematic diagram of the band structures for (a) n-type modulation-doped and (b) p-type modulation-doped $InP/In_xGa_{1-x}As$ heterostructures.

n-type $InP/In_xGa_{1-x}As$ structures

Figure 2 shows PL spectra of n-type samples at 2 K for different excitation intensities. Two broad emission bands (A_1 and A_2) appear at low excitation intensity conditions. With increased excitation intensity a third emission band (A_3) starts to gain intensity. Since any emission from the InP layer is located at much higher photon energy, the emissions observed must originate from the 500-Å active $In_xGa_{1-x}As$ layer. The most likely recombination processes are given in Fig. 1(a), i.e., A_1, A_2, and A_3 are related to recombination between the $n=1$, $n=2$, and $n=3$ 2D electron states and the $n=1$

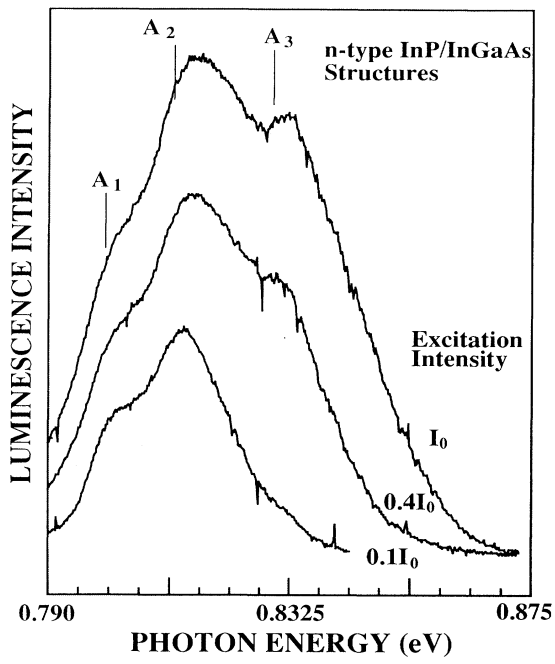

FIG. 2. PL spectra of n-type modulation-doped $InP/In_xGa_{1-x}As$ structures measured at varying excitation intensity levels.

heavy-hole state, respectively.

PL spectra have also been measured in the presence of a magnetic field. Figure 3(a) shows the PL spectra at three different magnetic fields, under the highest excitation intensity condition used in Fig. 2. Landau-level splitting is clearly resolved at magnetic fields above 2.5 T. The Landau-level numbers for the electrons and holes are used to indicate the corresponding transitions in Fig. 3. For example, 0-0 is the transition from the zero electron Landau level to the zero hole Landau level, while n, n', and n'' denote the nth Landau level related to the first, second, and third electron confined state, respectively.

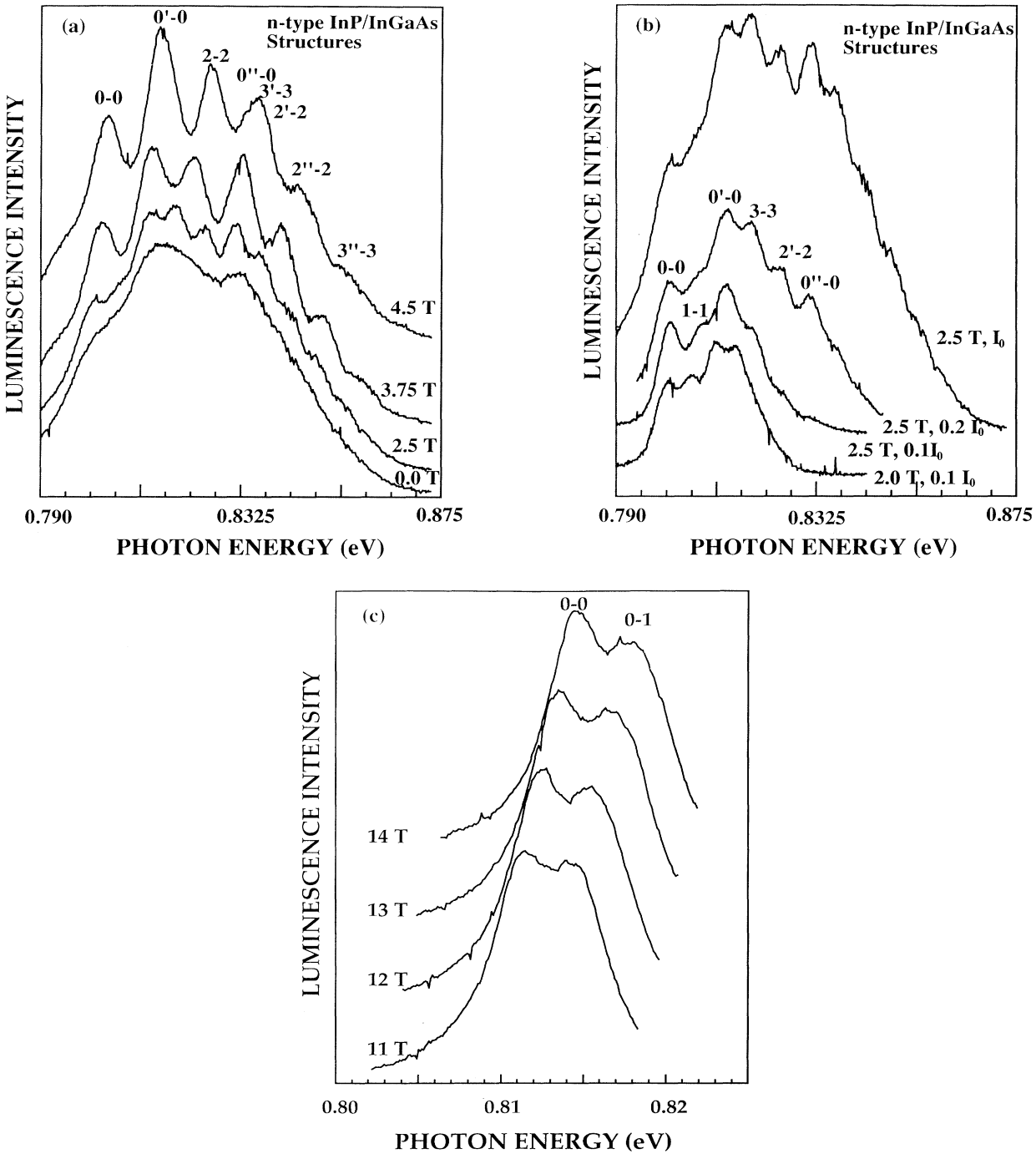

FIG. 3. (a) PL spectra of the n-type modulation-doped InP/$In_xGa_{1-x}As$ structures measured at different magnetic fields. The excitation intensity corresponds to the I_0 level used in Fig. 2. (b) PL spectra measured on the same sample as (a). The three upper curves have been measured at 2.5 T with different excitation intensity level. The two lower curves are measured at the same excitation intensity level, but at different magnetic fields. (c) PL spectra measured in the high magnetic-field region (11–14 T), covering only the transitions related to the zero Landau level of the $n=1$ confined electron state.

The lower the excitation intensity used, the better resolved is the Landau-level splitting observed at low fields. In Fig. 3(b), the three upper curves show PL spectra measured at 2.5 T at different excitation intensity levels. The lowest curve is a PL spectrum measured at 2.0 T at the lowest excitation intensity used in these measurements. The 1-1 transition is much better resolved at lower excitation intensity, while higher electronic states and transitions including higher Landau levels are better observed at higher excitation intensity. At high magnetic fields, the splitting between the transition 0-0 and 0-1 is observed [see Fig. 3(c)]. This splitting is a pure heavy-hole Landau-level splitting, from which the effective mass of heavy holes can be directly derived. In Fig. 4, all Landau-level splittings observed with different excitation intensities are summarized. It is obvious from Fig. 4 that all Landau levels converge into three transitions at zero magnetic field, which clearly demonstrates that the three emissions observed at zero magnetic field are all related to three different 2D-related levels. The energy levels of 2D carriers in a magnetic field parallel to the confinement direction (here referred to as the z direction) are given by

$$E_{n,m}=E_n+(m+\tfrac{1}{2})\hbar\omega_c=E_n+(m+\tfrac{1}{2})\frac{\hbar eH_z}{m^*} \quad (1)$$

with $m=0,1,2,\ldots$. Here E_n is the confined energy associated with the z motion of the carrier, H_z is the magnetic field along the z direction, and m^* is the reduced mass of the carriers involved in the transitions. The reduced mass m^*, deduced from a fitting of the experimental data by using Eq. (1), is estimated to be $m^*=(0.049\pm0.005)m_0$, and is defined by the following expression:

$$\frac{1}{m^*}=\frac{1}{m_e}+\frac{1}{m_{\rm hh}} . \quad (2)$$

Here m_e and $m_{\rm hh}$ are the effective masses of the electron and the heavy hole, respectively.

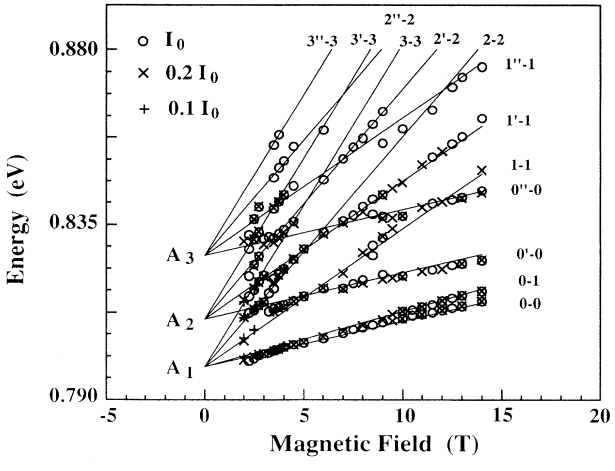

FIG. 4. Laudau-level splitting for the n-type modulation-doped InP/$In_xGa_{1-x}As$ structures. The points correspond to our experimental results, while the solid lines show the calculated Landau-level position according to Eq. (1).

In the high magnetic-field region (>8 T) the transition at the lowest energy splits into two components [see Figs. 3(c) and 4], which originate from pure heavy-hole Landau-level splitting. The importance of this observation is that the effective mass of the heavy holes can be independently deduced. The energy separation corresponding to the heavy-hole Landau-level splitting is equal to

$$\Delta E=\frac{e\hbar H_z}{m_{\rm hh}} . \quad (3)$$

By fitting the splitting observed, we obtain an effective-mass value of the heavy hole $m_{\rm hh}=(0.463\pm0.005)m_0$. This result is consistent with previous reports for epitaxial $In_xGa_{1-x}As$.[21,22]

With the experimentally determined reduced mass and the heavy-hole effective mass, we can evaluate the effective mass of the electron by using Eq. (2). The so-obtained value on the electron effective mass is $m_e=(0.054\pm0.005)m_0$.

The energy positions of the three transitions observed at zero field (A_1, A_2, and A_3) are 0.7984, 0.8108, and 0.8271 eV, respectively, which are deduced from the convergence of the Landau-level splitting at zero field. Accordingly, the energy separation $E_{12}=A_2-A_1=12.5$ meV is smaller than $E_{23}=A_3-A_2=16.2$ meV. This fact implies that the E_1 and E_2 levels originate from the opposite interfaces, as shown in Fig. 1(a) for the n-type samples. If the electronic levels had been located at the same interface, E_{23} should be smaller than E_{12}.[23,24] Consequently, the two low-energy emissions observed are related to the lowest electron levels confined at the opposite interfaces. The third emission is related to the next confined electronic level, as shown in Fig. 1. The Landau-level splitting follows the expected linear relationship with increasing magnetic field. No strong deviation from this relationship is observed up to 14 T, which indicates that the transitions observed are related to direct band-to-band transitions between confined electron states and hole states in the valence band. No significant exciton effects are observed in these transitions, even for the highest transition energies observed in this study. This means that the electron density remains well above the limit for the quenching of excitons due to phase-space filling and exchange effects.[25,26]

The structure studied provides a nice system for investigation of the dependence of the effective mass on the sublevel occupancy. In fact, some difference for the effective masses of electrons originating from different sublevels (up to $n=3$) are observed within our experimental accuracy. For the transitions 0′-0 (related to $n=2$) and 0″-0 (related to $n=3$), there is some deviation from the predicted behavior by using the same electron effective mass as used for the $n=1$ electron sublevel. This fact implies that the electron effective mass increases slightly for higher electron states. Particularly for the 0′-0 transition since the energy position of transition 0′-0 is well separated from other Landau-level transitions in optical spectra, a pronounced deviation is observed. The effective mass of $n=2$ subband electrons is found to be

about 9% larger than the effective mass of the $n=1$ electron state.

Comparing with previous studies,[7,8] our sample shows more well-defined Landau-level transitions, which allows us to deduce the effective masses more accurately. In addition, the well-resolved Landau-level splitting has made it possible to determine the effective masses of electrons and holes simultaneously.

p-type InP/$In_xGa_{1-x}As$ structures

Similar transitions are observed for the *p*-type modulation-doped structures as for the *n*-type structures. Figure 5 shows the PL spectra measured at different magnetic fields with the same excitation intensity condition as used in Fig. 3. Emission bands appearing at zero magnetic field split into Landau-level transitions with increasing magnetic field. The notations used in Fig. 5 are the same as used in Fig. 3, e.g., 1-1′ corresponds to the transition between the first electron Landau level and first hole Landau level related to the second hole subband. The magnetic-field dependence of the emissions is summarized in Fig. 6. All emissions observed at higher magnetic fields converge to two states at zero field (H_1,H_2). The energy separation between these two emissions measures to $H_2-H_1=6.9$ meV, which is much less than the corresponding difference for the electron subbands observed for the *n*-type structures. This is reasonable since the heavy-hole mass is much larger than the electron mass. The reduced mass obtained from a fitting of the Landau-level splitting in Fig. 6 is $(0.049\pm0.005)m_0$. This is the same value as obtained for the *n*-type structures, which is expected since the same electronic particles, i.e., the electron and heavy hole, are involved in the transition. The pure heavy-hole Landau-level splitting is observed also for the *p*-type structures (see Fig. 6). The splitting between the two components in the presence of a magnetic field is the same as observed in the *n*-type structures.

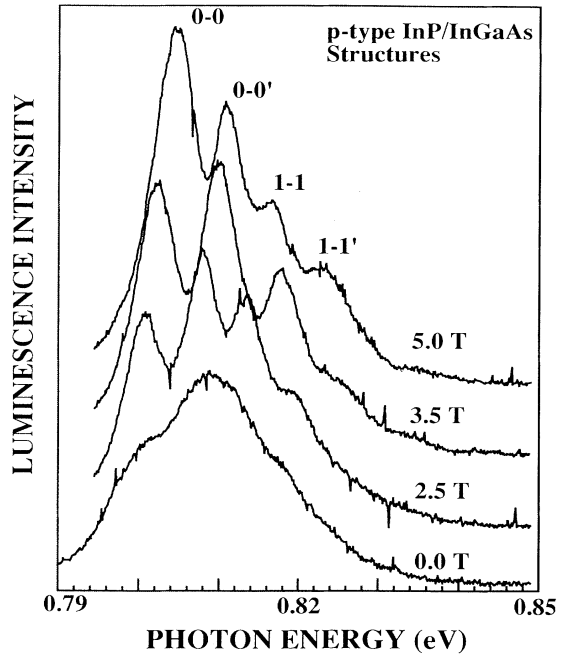

FIG. 5. PL spectra of *p*-type modulation-doped InP/$In_xGa_{1-x}As$ structures measured at different magnetic fields. The excitation conditions are the same as used in Fig. 3(a).

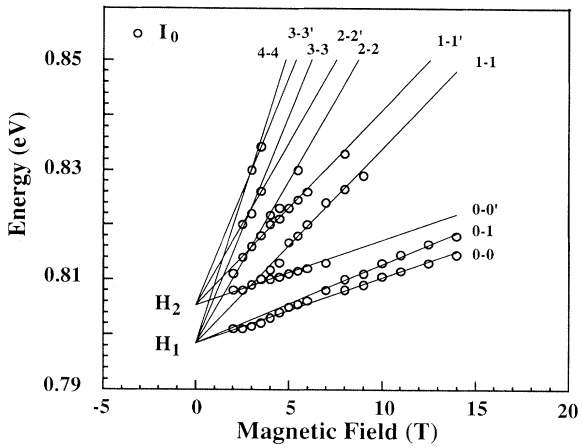

FIG. 6. Landau-level splitting for the *n*-type modulation-doped InP/$In_xGa_{1-x}As$ structures. The points correspond to our experimental results, while the solid lines show calculated Landau-level position according to Eq. (1).

It is important to note that the heavy-hole effective mass obtained in this study is fairly similar to the effective-mass value $m_{hh}=0.47m_0$ in the epitaxial $In_{0.53}Ga_{0.47}As$ material, while the electron effective mass deduced in this study is larger than the commonly used value.

For the *n*-type structures, photon-created holes are weakly confined in the center of the active layer, and the effective mass of the holes should be similar to the bulk value in analogy with observations made for the $Al_xGa_{1-x}As/GaAs$ heterostructures.[27] For our *p*-type structures, the confinement effect is more pronounced, since the holes are confined at one interface. In theory the hole effective mass should be different from the bulk value, when the holes experience confinement. However, in the recent magneto-optical studies[28] on $In_xGa_{1-x}As/In_xGa_{1-x}AsP$ 40- and 70-Å multiple quantum wells, the effective mass was estimated to be $0.55m_0$ and $0.45m_0$ for the $n=1$ and the $n=2$ heavy-hole states, respectively. This estimate is consistent with our results, $m_{hh}=(0.463\pm0.005)m_0$. In the pure 2D case, the in-plane mass of the heavy hole (at $k=0$) is predicted to be significantly smaller than the perpendicular mass. However, in real structures the system cannot be treated as pure 2D. The effective-mass value is influenced by the mixing of the light-hole and heavy-hole states, and the wave-function leakage into the barriers. These effects would result in an increase of the effective-mass value. Particularly, the effective mass of heavy holes away from $k(x,y)=0$ will increase, and can be larger than the perpendicular heavy-hole effective mass. According to theoretical calculations[30–32] on *p*-type $GaAs/Al_xGa_{1-x}As$ heterojunctions, the effective mass of spin-up heavy holes is dependent on the carrier concen-

trations, and is much larger than for the spin-down heavy-hole state. The in-plane effective mass of spin-up heavy hole varies from about $0.12m_0$ to $0.6m_0$ when the wave vector $k(x,y)$ is changed from zero to about 2.3×10^6 cm^{-1}.[32] The experimental effective-mass values in $Al_xGa_{1-x}As/GaAs$ structures with 5×10^{-11} cm^{-2} hole densities were found to be $0.6m_0$ and $0.38m_0$ for spin-up and spin-down heavy holes, respectively.[33] Accordingly, our rather large value obtained for the in-plane heavy-hole mass is not surprising. However, why a similar value for the effective hole mass is obtained for both n-type and p-type structures is not clear. To fully understand our results, detailed theoretical calculations of effective masses in our system have to be carried out, which is beyond the scope of this paper.

It is unambiguous that the effective mass of electrons confined in $InP/In_{0.53}Ga_{0.47}As$ structures deviates from the value derived from an interpolation between bulk GaAs and bulk InAs.[20] However, the dependence of the effective mass on the In concentration and the confinement in the $InP/In_xGa_{1-x}As$ heterostructures is still an open question. In particular, the influence of the carrier density on the electron mass is uncertain. We deduce an electron effective-mass value of $m_e=0.054m_0$, which is much larger than the commonly used value, $m_e=0.041m_0$. This discrepancy is currently not understood, and systematic experimental and theoretical studies are needed to understand the dependence of the effective mass on the material composition, the electron density, and the 2D confinement. However, theoretical calculations on $GaAs/Al_xGa_{1-x}As$ structures show that the in-plane effective mass of the confined electrons is drastically enhanced compared with GaAs bulk material.[29] From these calculations, it is also concluded that the enhancement of the electron in-plane effective mass is much stronger than in the perpendicular direction. Such a strong enhancement is explained in terms of nonparabolicity of the conduction band, the penetration of the wave function into the barriers, and the confinement energy. All these effects must also be taken into account for the $InP/In_{0.53}Ga_{0.47}As$ system. Therefore, the obtained enhancement of the electron effective mass compared to the bulk value is qualitatively expected.

SUMMARY

In summary we have presented magneto-optical studies of both n-type and p-type unstrained modulation-doped $InP/In_{0.53}Ga_{0.47}As$ heterostructures. Radiative recombination emissions related to 2D carriers are measured. For the n-type modulation-doped sample, the band-to-band transitions involving higher confined electron levels up to the $n=3$ level are observed. For the p-type modulation-doped sample, band-to-band transitions involving confined heavy-hole levels up to the $n=2$ level appear in PL spectra. The Landau-level splitting is well resolved both for n-type and p-type samples. Effective masses of electrons and holes are deduced simultaneously from the same measurements for the first time, to the best of our knowledge. The obtained values on the first subband electron effective mass is $m_e=(0.054\pm0.005)m_0$, and on the first subband heavy-hole effective mass is $m_{hh}=(0.463\pm0.005)m_0$. The effective mass of $n=2$ subband electrons was found to be about 9% larger than the effective mass of the $n=1$ electron subband.

[1]I. V. Kukushkin, K. v. Klitzing, and K. Ploog, Phys. Rev. B **37**, 8509 (1988).

[2]Q. X. Zhao, P. Bergman, P. O. Holtz, B. Monemar, C. Hallin, M. Sundaram, J. L. Merz, and A. C. Gossard, in *Impurities, Defects and Diffusion in Semiconductors: Bulk and Layered Structures,* MRS Symposia Proceedings No. 163, edited by Donald J. Wolford, Jerzy Bernholc, and Eugene E. Haller (Materials Research Society, Pittsburgh, 1989), p. 337; Q. X. Zhao, J. P. Bergman, P. O. Holtz, B. Monemar, K. Ensslin, M. Sundaram, J. L. Merz, and A. C. Gossard, Superlatt. Microstruct. **9**, 161 (1991).

[3]Q. X. Zhao, J. P. Bergman, P. O. Holtz, B. Monemar, C. Hallin, M. Sundaram, J. L. Merz, and A. C. Gossard, Semicond. Sci. Technol. **5**, 884 (1990).

[4]Q. X. Zhao, Y. Fu, P. O. Holtz, B. Monemar, J. P. Bergman, K. A. Chao, M. Sundaram, J. L. Merz, and A. C. Gossard, Phys. Rev. B **43**, 5035 (1991).

[5]J. P. Bergman, Q. X. Zhao, P. O. Holtz, B. Monemar, M. Sundaram, J. L. Merz, and A. C. Gossard, Phys. Rev. B **43**, 4771 (1991).

[6]Q. X. Zhao, P. O. Holtz, B. Monemar, E. Sörman, C. Hallin, M. Sundaram, J. L. Merz, and A. C. Gossard, Phys. Rev. B **46**, 4352 (1992).

[7]D. G. Hayes, M. S. Skolnick, D. M. Whittaker, P. E. Simmonds, L. L. Taylor, S. J. Bass, and L. Eaves, Phys. Rev. B **44**, 3436 (1991).

[8]P. E. Simmonds, M. S. Skolnick, L. L. Taylor, S. J. Bass, and K. J. Nash, Solid State Commun. **67**, 1151 (1988).

[9]M. Razeghi, S. P. Hirtz, U. O. Ziemelis, C. Delaude, R. Etienne, and M. Voos, Appl. Phys. Lett. **43**, 585 (1983).

[10]H. Temkin, M. B. Panish, P. M. Petroff, R. A. Hamm, J. M. Vandenberg, and S. Samski, Appl. Phys. Lett. **47**, 394 (1985).

[11]M. S. Skolnick, L. L. Taylor, S. J. Bass, A. D. Pitt, D. J. Mowbrag, A. G. Cullis, and N. G. Chew, Appl. Phys. Lett. **51**, 24 (1987).

[12]W. T. Tsang and E. F. Schubert, Appl. Phys. Lett. **49**, 220 (1986).

[13]Yoshihiro Kawaguchi and Hajime Asahi, Appl. Phys. Lett. **50**, 1243 (1987).

[14]D. Gershoni, H. Temkin, and M. B. Panish, Phys. Rev. B **38**, 7870 (1988).

[15]Mitsuru Sugawara, Phys. Rev. B **45**, 11 423 (1992).

[16]M. S. Skolnick, J. M. Rorison, K. J. Nash, D. J. Mowbray, P. R. Tapster, S. J. Bass, and A. D. Pitt, Phys. Rev. Lett **58**, 2130 (1987).

[17]*GaInAsP Alloy Semiconductors,* edited by T. P. Pearsall (Wiley, New York, 1982).

[18]*Semiconductors,* edited by O. Madelung, M. Schulz, and H. Weiss, Landolt-Börnstein, New Series, Group III, Vol. 17a (Springer, Berlin, 1982).

[19]S. R. Forrest, P. H. Schmidt, R. B. Wilson, and M. L. Kaplan, Appl. Phys. Lett. **45**, 1199 (1984).
[20]C. Wetzel, Al. L. Efros, A. Moll, B. K. Meyer, P. Omling, and P. Sobkowicz, Phys. Rev. B **45**, 14 052 (1992).
[21]K. H. Goetz, D. Bimberg, A. V. Solomonov, G. F. Glinski, and M. Razeghi, J. Appl. Phys. **54**, 4543 (1983).
[22]K. Alavi and R. L. Aggrawal, Phys. Rev. B **21**, 1311 (1980).
[23]T. Ando, J. Phys. Soc. Jpn. **51**, 3900 (1982).
[24]G. Bastard, Surf. Sci. **142**, 284 (1984).
[25]G. Livescu, D. A. B. Miller, D. S. Chemla, M. Ramaswamy, T. Y. Chang, N. Sauer, A. C. Gossard, and J. H. English, IEEE J. Quantum Electron. **24**, 1677 (1988).
[26]D. Huang, H. Y. Chu, Y. C. Chang, R. Houdré, and H. Morkoç, Phys. Rev. B **38**, 1246 (1988).
[27]I. V. Kukushkin, K. v. Klitzing, and K. Ploog, Phys. Rev. B **37**, 8509 (1988).
[28]S. L. Wong, R. J. Nicholas, C. G. Cureton, J. M. Jowett, and E. J. Thrush, Semicond. Sci. Technol. **7**, 493 (1992).
[29]U. Ekenberg, Phys. Rev. B **40**, 7714 (1989).
[30]T. Ando, J. Phys. Soc. Jpn. **54**, 1528 (1985).
[31]D. A. Broido and L. J. Sham, Phys. Rev. B **31**, 888 (1985).
[32]E. Bangert and G. Landwehr, Superlatt. Microstruct. **1**, 363 (1985).
[33]H. L. Störmer, A. Chang, Z. Schlesinger, D. C. Tsui, A. C. Gossard, and W. Wiegmann, Phys. Rev. Lett. **51**, 126 (1983).